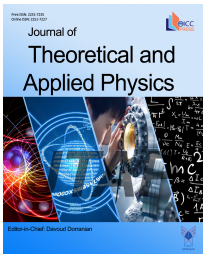

Volume 19, Issue 3, 192533 (1-8)

Journal of Theoretical and Applied Physics (JTAP)

https://doi.org/10.57647/j.jtap.2025.1903.33

Low frequency domain analysis of alternating magnetic flux leakage method

Hamid Eftekhari[1,*], Mohammad Mehdi Tehranchi[2,3]

[1]*Department of physics, SR.C, Islamic Azad University, Tehran, Iran.*
[2]*Laser and Plasma Research Institute, Shahid Beheshti University, Tehran, Iran.*
[3]*Physics Department, Shahid Beheshti University, Tehran, Iran.*

[*]**Corresponding author:** h.eftekhari@iau.ac.ir

Original Research

Received:
10 May 2025
Revised:
15 June 2025
Accepted:
26 June 2025
Published online:
30 June 2025

Abstract:

Alternating Magnetic Flux Leakage method was used to investigate the relation between the leaked magnetic field and crack dimension by changing the frequency of the magnetic field induced in the specimen. In this way, the alternating magnetic field with frequency in range of $1-100$ Hz was induced into a defective ferromagnetic steel plate and the magnetic field over the surface was measured. Then, two sensors in differential modes were used to extract the effect of frequency on the relative Magnetic Flux Leakage signal. The results indicated that the frequency of minimum of the relative Magnetic Flux Leakage increases linearly by increasing the crack depth. The experimental results were verified by numerical finite element simulation method.

Keywords: Magnetic flux leakage; Low frequency; Sensors

1. Introduction

The Magnetic Flux Leakage (MFL) method is considered as one of the mostly-used method in Non Destructive Testing (NDT) in oil and gas pipeline and tank inspection [1–6]. In this method, a ferromagnetic sample was magnetized with an external magnetic field. Around the defect, the magnetic field leaked from the sample to the air is related to the discontinuity in the magnetic properties of the sample. This leaked magnetic field is proportional to the defect profile [7–13].

The MFL method was developed in Direct Current Magnetic Flux Leakage (DCMFL) [14–16], Alternating Current Magnetic Flux leakage (ACMFL) [17–20] and Pulsed Magnetic Flux Leakage (PMFL) [21, 22] by using different types of magnetic field excitation.

In DCMFL, the sample is magnetized to near saturation with a static magnetic field. In the defect location, the magnetic field leaks to the air. The location and properties of the defect could be characterized by measuring this leaked magnetic field.

Sophian et al. proposed pulsed magnetic flux leakage (PMFL) techniques. This method has the advantage of detecting deeper subsurface defects, locating and sizing defects [23].

Among the MFL methods, the ACMLF method for the surface defects is more sensitive than the two other methods due to the skin depth of the applied alternating magnetic field [24–27]. In ACMFL, the frequency dependency of the MFL signal could illustrate the relation between the skin effect and crack dimensions due to the crack dimension. The axial cracks could be detected by using the ACMFL [24]. Wu et al. used a composite of DCMFL and ACMFL to detect the longitudinal and axial cracks [26]. Rongbiao et al. indicated that AC and DC composite magnetization detect both external and internal defects [27].

In among of crack parameters, the crack depth is more important in oil and gas industries, however the ACMFL method due to the skin effect is less sensitive to the crack depth [13–16].

In this paper, an alternating magnetic field was used to excite the MFL signal of a cracked ferromagnetic plate. By applying two Hall Effect sensors, the magnetic field leaked

from the crack and surface of the specimen was measured and the effect of frequency on the MFL signal was studied. Experimental data were verified by the simulated data obtained by Finite Element Method Packages. The results showed that this method is more sensitive to the crack depth, less sensitive to the crack length, and more easy to use.

2. Experimental procedure

In this study, four different magnetic steel plates with the dimensions of $9 * 250 * 100$ mm were used, each of which included the cracks with the same width and length of 1 mm and 10 mm, respectively, and different depths of 3, 4, 5 mm. The samples were magnetized with a U shape magnetic yoke and 2 electric coils each had 1 ampere peak current and 250 turns. The AC current of the coils was introduced by the function generator and amplified by La6500 power operational amplifier.

In the next procedure, the X component of MFL signal was measured by a Hall effect sensor. The Perkin-Elmer 7265 Lock-In-Amplifier was used to increase the signal to noise ratio. All of the experimental setup was controlled by the PC. Fig. 1 displays a schematic diagram of the setup.

3. Simulation procedure

The experimental data was simulated by Comsol Multiphysics modeling software. In addition, a 3D Finite Element Method (FEM) model was built as shown in Fig. 2. To increase the accuracy of the simulation, the mesh size decreased around the crack and increased in region, which is far from the crack. Table 1 shows mesh parameters in comsol simulation.

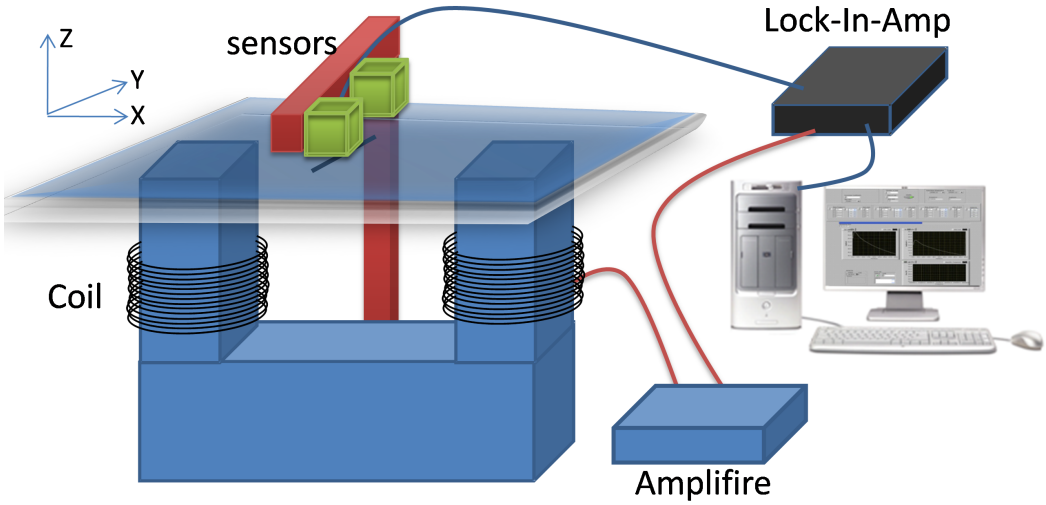

Figure 1. A schematic diagram of the experimental procedure.

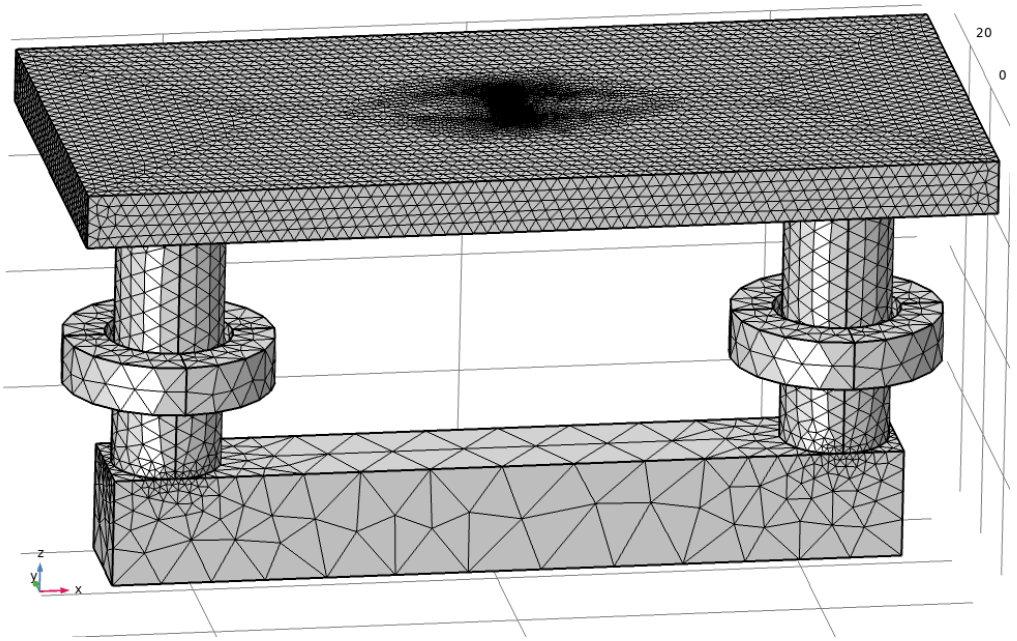

Figure 2. Simulation model and mesh sizes.

Table 1. Mesh parameters used in simulation.

	Min (mm)	Max (mm)	Grow rate
Crack	0.09	0.25	1.35
Specimen	0.13	3.1	1.2
Yoke	0.88	12.1	1.4
Air	0.8	18	1.4

Regarding the specimen and magnetic Yoke, soft iron (with losses) is used with the B-H curve and relative permeability as shown in Fig. 3.

4. Results and discussion

The set of coils, magnetic yoke, and specimen have the total inductance L and impedance Z by using the following equation [28]:

$$Z = \sqrt{r^2 + L^2\omega^2}, \quad \tan\theta = \frac{L\omega}{r}, \quad \omega = 2\pi\nu \tag{1}$$

In this set, when an alternating sinusoidal voltage is applied to the coils, the electrical current passed through the coils is expressed as follows:

$$I = \frac{V}{Z} = \frac{V}{\sqrt{r^2 + 4\pi^2 L^2 \nu^2}} \tag{2}$$

Increasing the ω results in decreasing the current. In addition, the r_{ac} increases with ω due to skin effect [29]. As shown in Fig. 4, the current amplitude in coils in constant voltage is demonstrated as a function of ν.
The fitted curve in Fig. 4 is obtained as follows:

$$I = \frac{2}{\sqrt{3.4 + 3.92\nu^{0.76}}} \tag{3}$$

Eqs. (2) and (3) show that the dependency of r_{ac} and L to ω change the simple relation between the I and ω. By decreasing the electric current against increasing the ω, the MFL signal above the specimen should be decreased as a function of ω.

By increasing the frequency, the current confined to the surface of the conductor in region called "skin depth" due to the eddy current. The skin depth is expressed as follows [29]:

$$\delta = \sqrt{\frac{\rho}{\pi\nu\mu_0\mu_r}} \approx 503\sqrt{\frac{\rho}{\mu_r\nu}} \ \text{(mm)} \tag{4}$$

where ρ indicates resistivity, μ_r shows relative magnetic permeability, and ν is considered as the frequency of alternating magnetic field. Regarding $\rho = 0.2 \times 10^{-6}$ (Ω.m) and $\mu_r = 800$, the skin depth as a function of frequency is shown in Fig. 5 (a). The slope of the curve changes in the vicinity of 6 Hz because the dependency of μ_r on the frequency of the magnetic field. Fig. 5 (b) shows the simulated result of MFL signal in 1 mm liftoff above the center of crack as a function of the frequency of magnetic field for different cracked samples with the same crack length of 10 mm, width of 1 mm, and depths of 3, 4 and 5 mm, as well as a sample without crack. Fig. 5 (c) displays the experimental data of Hall sensor output, which placed 1 mm above the center of crack for different crack depths of $3-5$ mm, as well as constant length and width of 10 mm and 1 mm, respectively.
By increasing the frequency from 1 to 20 Hz, the leaked magnetic field over the surface decreases rapidly, and then the MFL signal changes slowly. By increasing the crack depth, the MFL signal increases in each frequency, although the increase is not equal for all of the frequencies. Decreasing the electric current strongly affected the MFL signal. Thus, the effect of the decrease in the current should be extracted to find the effect of crack depth on the MFL fre-

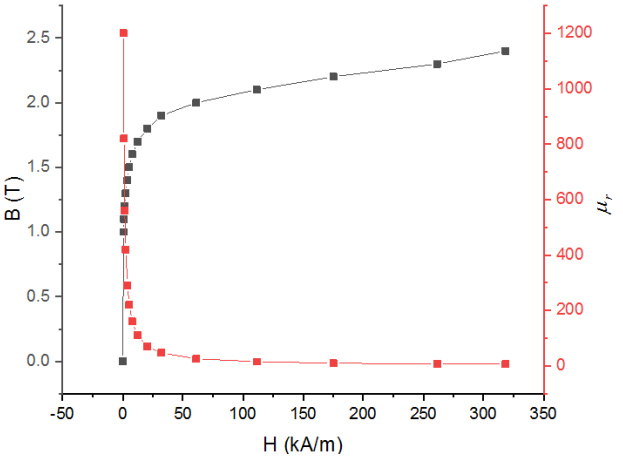

Figure 3. B-H curve and relative permeability of the materials used as specimen and magnetic Yoke in simulation.

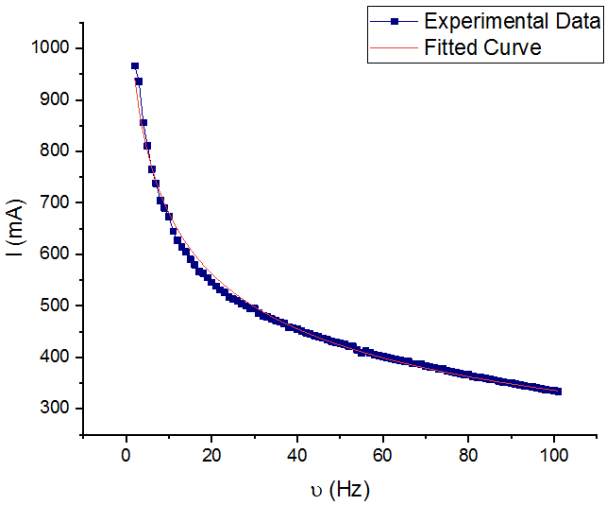

Figure 4. The electric current passed through the coils.

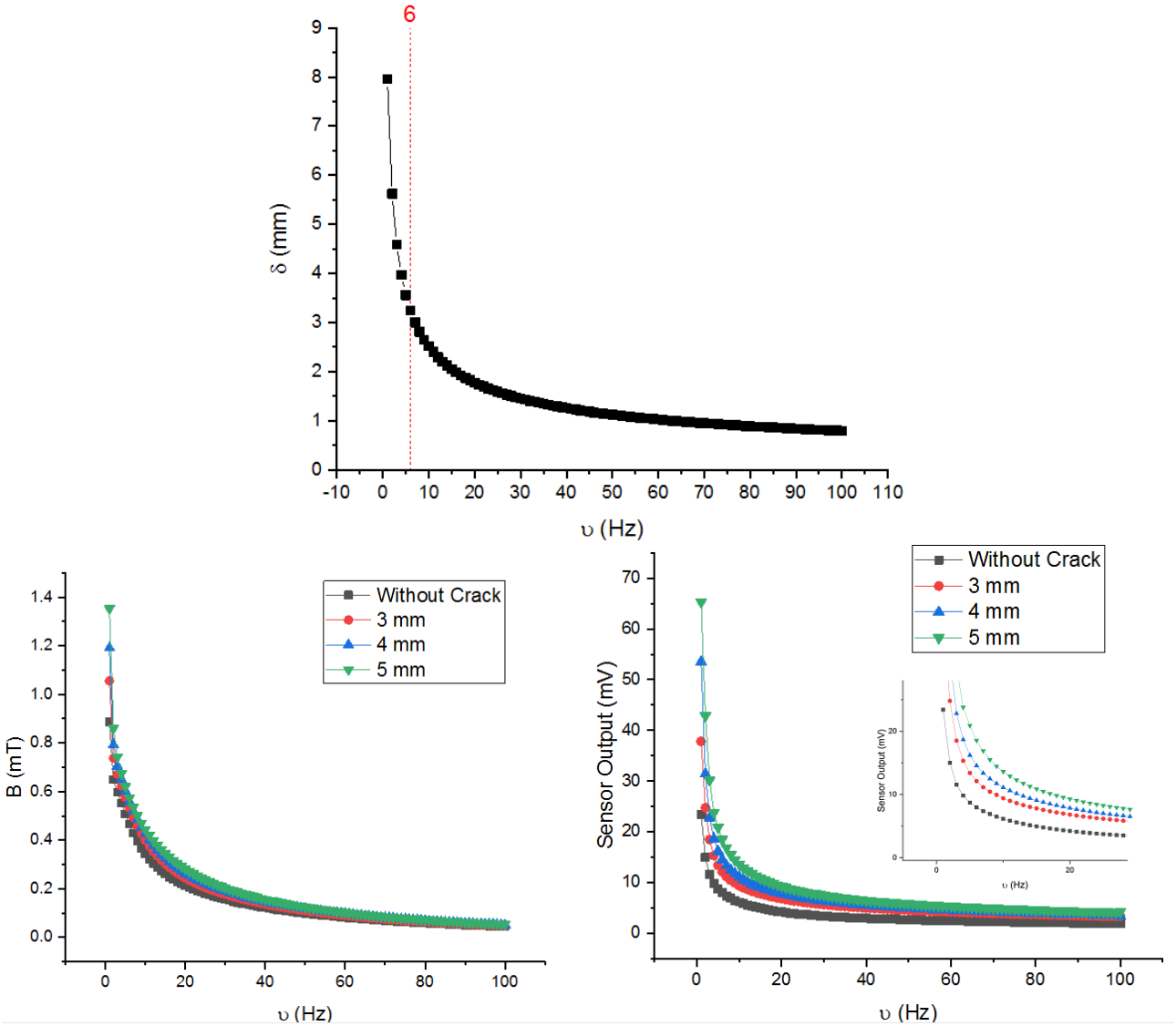

Figure 5. (a) The skin depth as a function of frequency, (b) Simulated result of MFL signal as the function of frequency for different 3 – 5 mm depths (left) and (c) Experimental data of magnetic sensor output for different depth in range of 3 – 5 mm (right).

quency dependency. To this aim, we use the Relative MFL (R-MFL) response based on the following equation:

$$\frac{\Delta R}{R}(\%) = \frac{R_{(\text{with Crack})} - R_{(\text{without Crack})}}{R_{(\text{without Crack})}} \times 100 \qquad (5)$$

where $R_{(\text{with Crack})}$ indicates the MFL response (or equally sensor output) upon the center of the crack and $R_{(\text{without Crack})}$ represents the MFL response (sensor output) upon the surface of the specimen without any crack. Eq. (5) removes the effect of decreasing and extracting the absolute response of the crack because decreasing the electric current leads to a decrease in $R_{(\text{with Crack})}$ like $R_{(\text{without Crack})}$. To measure $R_{(\text{with Crack})}$ and $R_{(\text{without Crack})}$ simultaneously, we used 2 sensors one over the crack and another in 10 mm far from the crack in the same X coordinate as shown in Fig. 1. The simulated and experimental results obtained by Eq. (5) for the crack depth from 3 to 5 mm are shown in Figs. 6 (a) and (b) respectively.

As shown, the R-MFL response decreases strongly to its minimum around 8 Hz and increase slowly by increasing the frequency, leading to a constant value. The R-MFL percentage increased by increasing the crack depth. Further, the depth of the well in the curve decreased by increasing the minimum of curve and fade in crack depth of 5 mm by increasing the crack depth. This relationship illustrated in Fig. 7 displays the change in well depth, frequency, and relative MFL percentage of the minimum in simulated and experimental conditions. In addition, the frequency of the minimum increased by increasing the crack depth. By increasing the crack depth, the R-MFL of the minimum in Fig. 6 increase straightly. As shown, a good relationship was observed between the simulated and experimental results.

Fig. 8 (a) displays the 6 Hz AC magnetic field in the plate near a crack with 5 mm depth when the angle (phase) is zero. As shown, the color of streamlines is consistent with the magnitude of magnetic field. Furthermore, the magnetic field is distorting near the crack since the crack is like a wall against the magnetic flux passed through the crack region. Thus, the magnetic flux is distorted and compressed to the

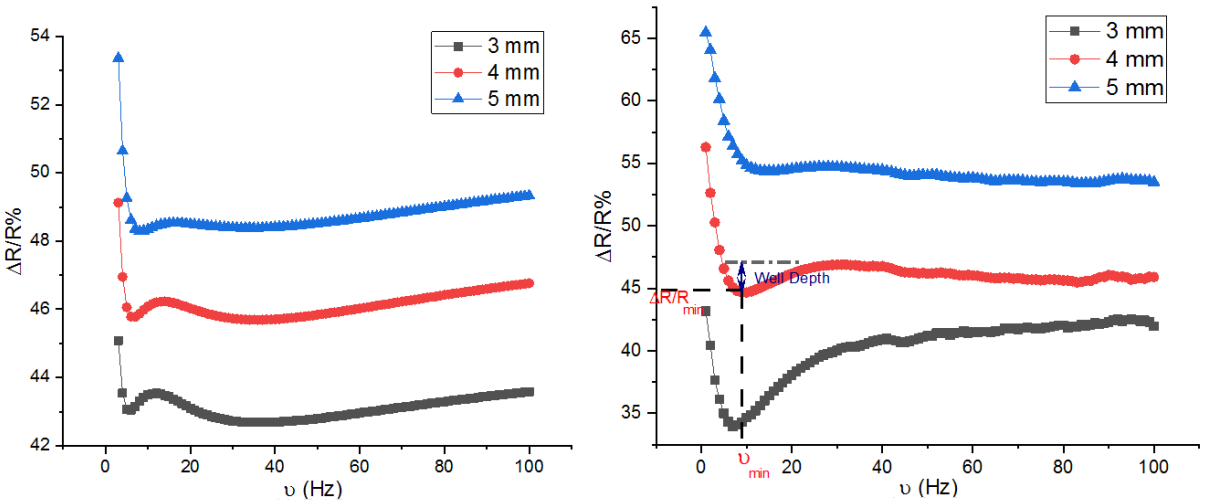

Figure 6. (a) The simulated and (b) Experimental results obtained by Eq. (5) for different crack depths from 3 to 6 mm.

remained region, which is denoted as L. The remaining region (L) decreases by increasing the crack Depth (D). At this phase, the magnetic field is going from left to right in skin depth however in vicinity of the sample the magnetic field (which has low amplitude) may flows in opposite direction due to the eddy current. Fig. 8 (b) displays simulated magnetic field along the L in Fig. 8 (a) at various frequencies. As shown the magnetic field decreased by increasing the frequency and near the surface the magnetic field increased.

The eddy current was induced in the specimen in order to oppose the change in the magnetic field since we induced an alternating magnetic field into the specimen due to the Lenz Law. In the present study, the magnetic field is in X direction and the eddy current induced is in Y direction (Fig. 1). Fig. 9 (a). shows the eddy current density induced in Y direction at the cross-section of the specimen around the crack with 4 mm depth at the frequency of 6 Hz when the phase is zero. The color of streamlines is related to the current density amplitude.

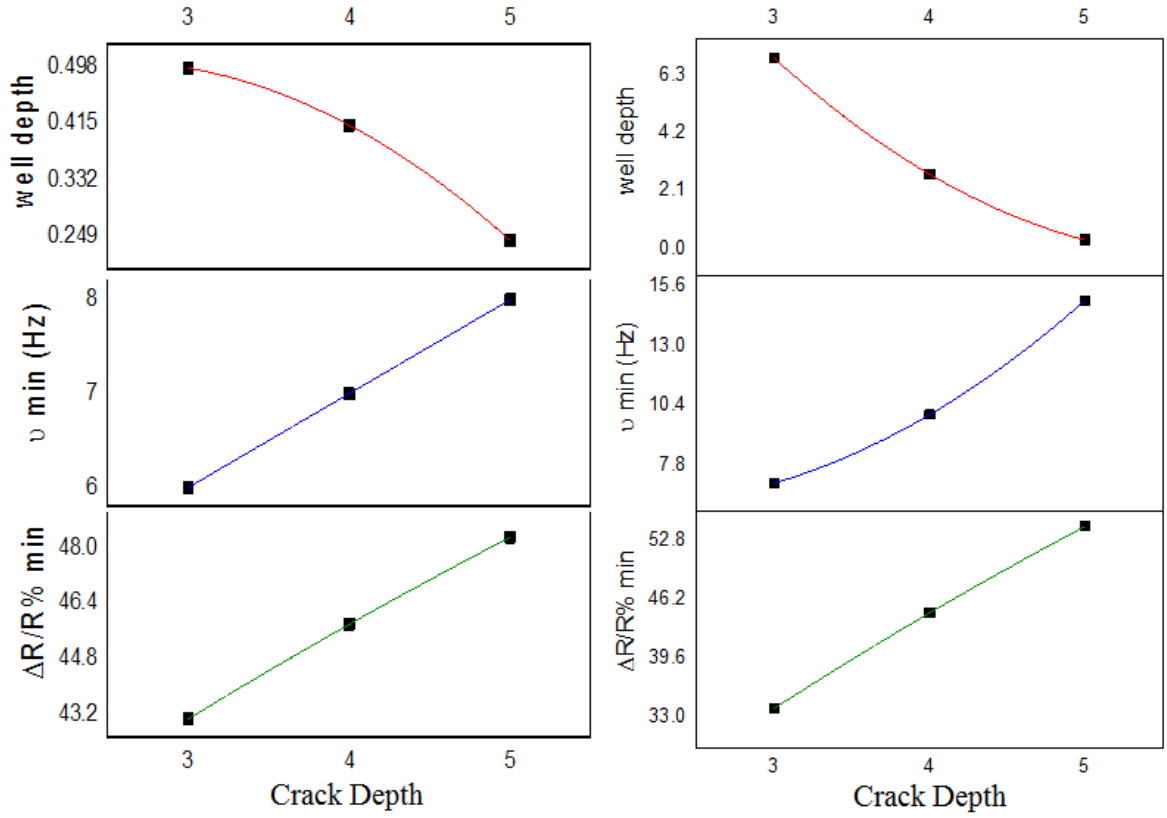

Figure 7. Well depth, frequency of minimum and R-MFL of minimum in the curve obtained from simulation (left) and experimental (right) results as the crack depth.

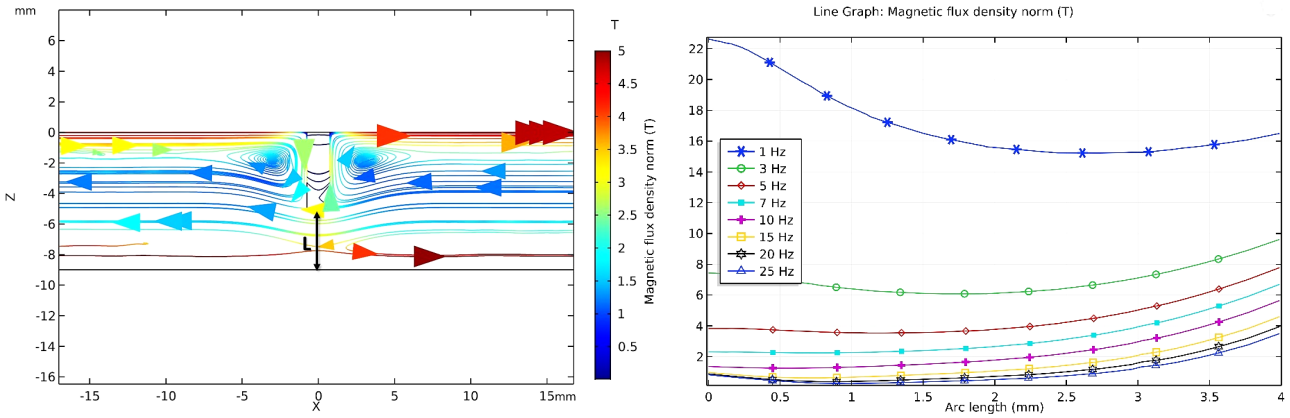

Figure 8. (a) Simulation of magnetic field inside the specimen near the crack at 6 Hz, and (b) Simulated magnetic field along the *L* in (a) at various frequencies.

The eddy current and magnetic field decreased in the center of the specimen and amplified in the amount of the surface called "skin depth" by increasing the frequency. The eddy current flow in clockwise direction and has small closed loop in right and left side of the crack. Fig. 9 (b) and 9 (c) show the simulated current density along the *L* in Fig. 9 (a) and current density in sample without the crack at different frequencies respectively. The negative magnitude means that the direction of current (magnetic field) is in an opposite.

In the sample without the crack, by increasing the frequency up to 10 Hz the current is going to the surface and decreases more than in bottom of the crack, while the current in bottom of the crack is almost constant. This effect leads to

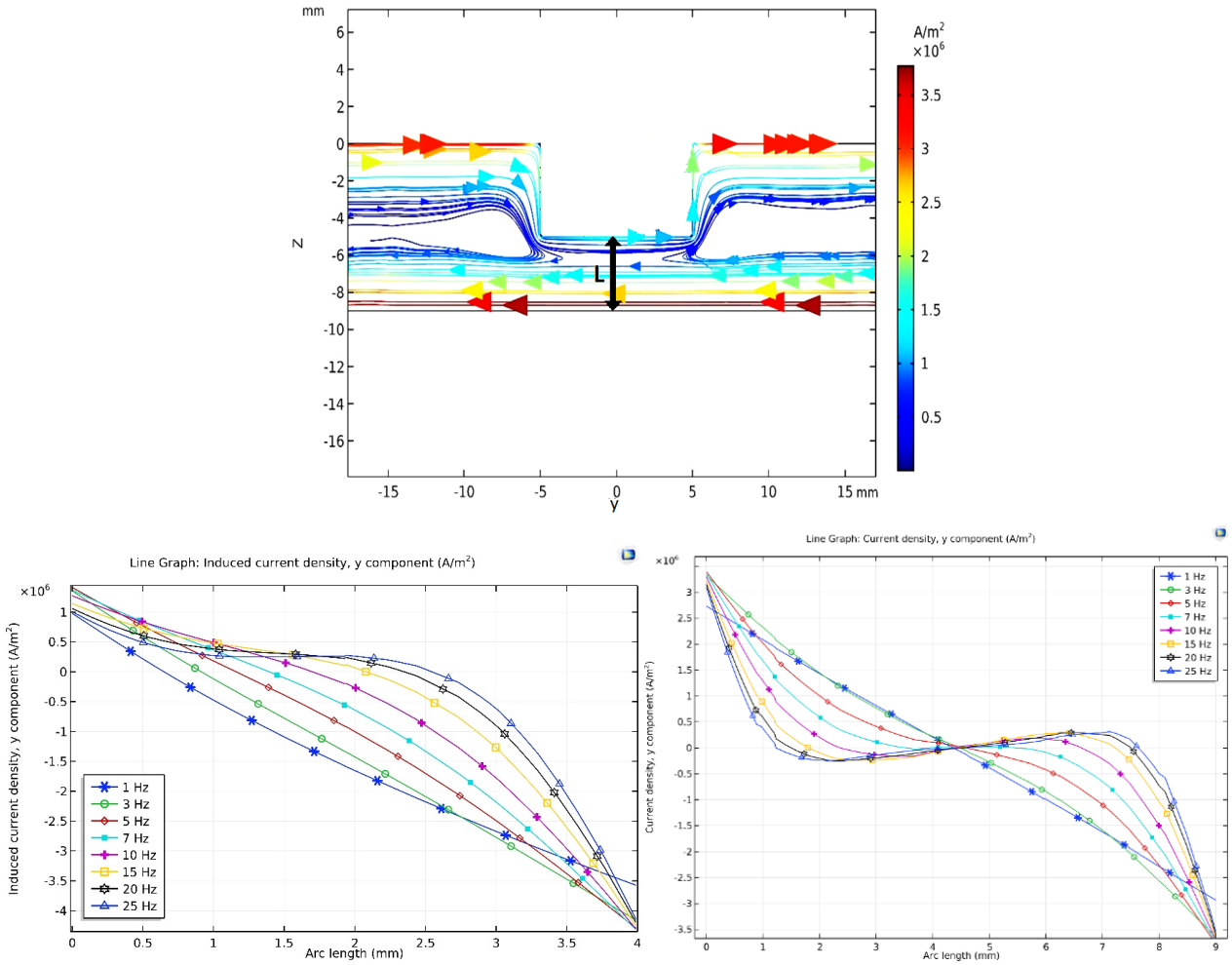

Figure 9. (a) The simulated induced eddy current density in Y direction at the cross-section near the crack at 6 Hz, (b) simulated eddy current along the blackline *L* in (a) at various frequencies (left), (c) eddy current in sample without the crack (right).

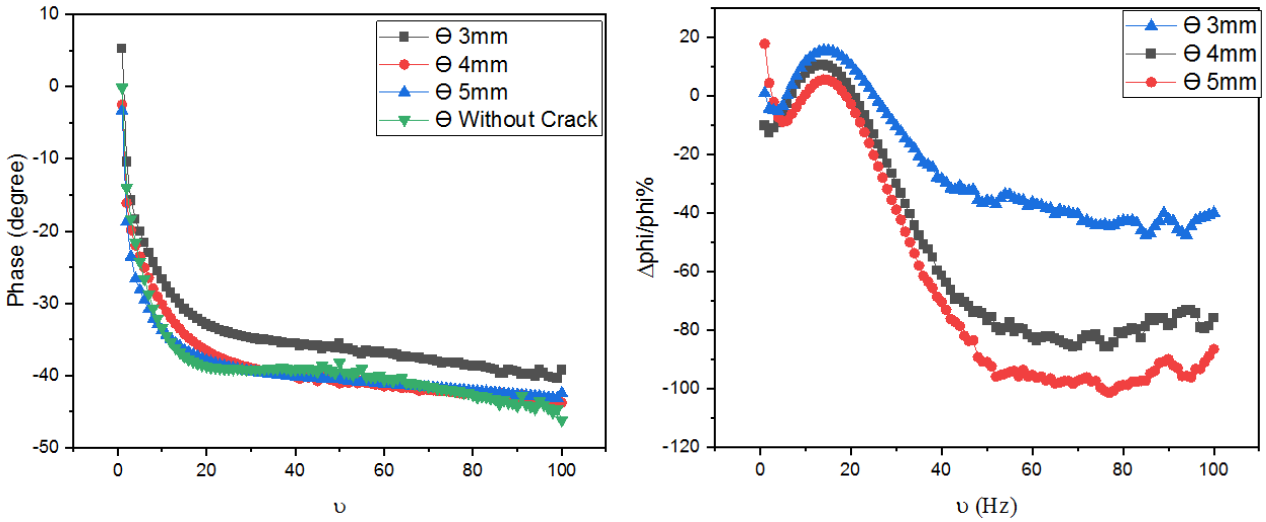

Figure 10. (a) Experimental result of phase of MFL signal as the function of frequency for different $3-5$ mm depths (left), (b) change of relative phase as the function of frequency obtained by equation 5 (right).

decreasing in *R*-MFL. In range of 10 Hz to 20 Hz, the current in bottom of the crack is going to the surface while in sample without the crack changing in distribution of the current against the frequency become slowly leads to increasing the *R*-MFL. In frequency more than 20 Hz, in both samples with and without the crack the current distribution changes slowly against the frequency. This effect cause that the *R*-MFl change slightly.

Based on the results, the skin depth is not symmetric in the bottom of the crack, however it is symmetric in the sample without the crack at the same position of the crack. This asymmetry increases by increasing the frequency.

Fig. 10 (a) displays the experimental data of phase of Hall sensor output as the function of frequency. The phase of sample which has crack is more than the sample without the crack and decrease rapidly in range of $1-20$ Hz. Fig. 10 (b) show the phase of *R*-MFL as the function of frequency. The relative phase shows more complicated behavior than the *R*-MFL (Fig. 6). By increasing the crack depth, the phase of *R*-MFL decreases in all frequency and change in phase as the function of crack depth increases by increasing the frequency.

5. Conclusion

The present study aimed to evaluate the effect of frequency on the behavior of the ACMFL response. To illustrate the effect of the frequency, we used relative-MFL which extracted the effect of reduction in excitation of magnetic field by increasing the frequency. Based on the results, the frequency dependency of *R*-MFL response changes by increasing the crack depth. Finally, *R*-MFL response and frequency of the minimum of the *R*-MFL increased linearly by increasing the crack depth. The experimental results were verified by the simulation results.

Authors Contribution
Authors have contributed equally in preparing and writing the manuscript.

Availability of data and materials
The data that support the findings of this study are available from the corresponding author upon reasonable request.

Conflict of interests
The authors declare that they have no known competing financial interests or personal relationships that could have appeared to influence the work reported in this paper.

References

[1] S. Huang and W. Zhao. "Magnetic Flux Leakage: Theories and Imaging Technologies.". De Gruyter, Berlin/Boston, 2016.

[2] M. Coramik and Y. Ege. "Discontinuity inspection in pipelines: A comparison review.". *Measurement*, 2017.
DOI: https://doi.org/10.1016/j.measurement.2017.07.058.

[3] D Zhang, E. Zhang, and S. Pan. "A new signal processing method for the nondestructive testing of a steel wire rope using a small device.". *NDT & E International*, 2020.
DOI: https://doi.org/10.1016/j.ndteint.2020.102299.

[4] X. Gao, Y. Li, X. Zhou, X. Dai, Y. Zhang, D. You, and N. Zhang. "Multidirectional magneto-optical imaging system for weld defects inspection.". *Optics and Lasers in Engineering*, 2020.
DOI: https://doi.org/10.1016/j.optlaseng.2019.105812.

[5] O. Zhang and X. Wei. "Analysis of MFL Model for Sucker Rod Defects and Its MFL Signal Processing.". *Journal of Testing and Evaluation*, 2019.
DOI: https://doi.org/10.1520/JTE20170687.

[6] Z. Zhou and Z. Liu. "Fault Diagnosis of Steel Wire Ropes Based on Magnetic Flux Leakage Imaging under Strong Shaking and Strand Noises.". *IEEE Transactions on Industrial Electronics*, 2020.
DOI: https://doi.org/10.1109/TIE.2020.2973874.

[7] Y. Egea, S. Bicakcıb, H. Gunesb, H. Citakc, and M. Coramik. "An application of BRANN and MFL methods: Determining crack type and physical properties on M5 steel sheets.". *Measurement*, 2019.
DOI: https://doi.org/10.1016/j.measurement.2019.02.064.

[8] J. Jingpin, S. Junjun, L. Nan, S. Guorong, W. Bin, and H. Cunfu. "Micro-crack detection using a collinear wave mixing technique.". *NDT & E International*, 2014.
DOI: https://doi.org/10.1016/j.ndteint.2013.12.004.

[9] Y. Ege and M. Coramik. "A new measurement system using magnetic flux leakage method in pipeline inspection.". *Measurement*, 2018.
DOI: https://doi.org/10.1016/j.measurement.2018.03.064.

[10] P. Deng, C. He, Y. Lyu, G. Song, J. Jiao, and B. Wu. "Detection of Inner Wall Circumferential Cracks in the Special-Shaped Pipes Using Surface Waves.". *Journal of Nondestructive Evaluation*, 2019.
DOI: https://doi.org/10.1007/s10921-018-0554-5.

[11] Z. Wei, F. Jianchun, L. Xiangyuan, and L. Shujie. "Quantitative research of defects for pipelines based on metal magnetic memory testing.". *Insight - Non-Destructive Testing and Condition Monitoring*, 2020.
DOI: https://doi.org/10.1784/insi.2020.62.5.292.

[12] S. C. Sood and G. Assimacopoulos. "NDE Welds Inspection Qualifications for Pipework and Pipelines.". *Sensor Letters*, 2014.
DOI: https://doi.org/10.1166/sl.2014.3302.

[13] G. Xiangdong, Z. Xiaohu, W. Congyi, M. Nvjie, Z. Yanxi, and Y. Deyong. "Skin depth and detection ability of magneto-optical imaging for weld defects in alternating magnetic field.". *Journal of Manufacturing Systems*, 2020.
DOI: https://doi.org/10.1016/j.jmsy.2020.02.006.

[14] M. M. Tehranchi and H. Eftekhari. "Miniaturized magneto-optical imaging sensor for crack and microcrack detection.". *Optik*, 2020.
DOI: https://doi.org/10.1016/j.ijleo.2019.163830.

[15] M. M. Tehranchi, S. M. Hamidi, H. Eftekhari, M. Karbaschi, and M. Ranjbaran. "The inspection of magnetic flux leakage from metal surface cracks by magneto-optical sensors.". *Sens. Actuators A Phys*, 2011.
DOI: https://doi.org/10.1016/j.sna.2011.09.010.

[16] M. M. Tehranchi, H. Eftekhari, and M. Ranjbaran. "Imaging Metal Surface Cracks with Giant Magnetoimpedance Sensor.". *Sensor Letters*, 2013.
DOI: https://doi.org/10.1166/sl.2013.2770.

[17] K. Tsukada et al. "Detection of Inner Cracks in Thick Steel Plates Using Unsaturated AC Magnetic Flux Leakage Testing With a Magnetic Resistance Gradiometer.". *IEEE Transactions on Magnetics*, 2017.
DOI: https://doi.org/10.1109/TMAG.2017.2713880.

[18] G. Xiangdong et al. "Elucidation of magnetic flux leakage for welding defect detection at different magnetic field directions through alternating magnetic field measurement.". *Insight-Non-Destructive Testing and Condition Monitoring*, 2019.
DOI: https://doi.org/10.1784/insi.2019.61.12.720.

[19] W. Lou et al. "Internal Defect Detection in Ferromagnetic Material Equipment Based on Low-Frequency Electromagnetic Technique in 20# Steel Plate.". *IEEE Sensors Journal*, 2018.
DOI: https://doi.org/10.1109/JSEN.2018.2850977.

[20] Y. Feng, L. Zhang, and W. Zheng. "Simulation analysis and experimental study of an alternating current field measurement probe for pipeline inner inspection.". *NDT & E International*, 2018.
DOI: https://doi.org/10.1016/j.ndteint.2018.04.015.

[21] R. Mardaninejad and M. S. Safizadeh. "Gas Pipeline Corrosion Mapping Through Coating Using Pulsed Eddy Current Technique.". *Russ J Nondestruct Test*, 2019.
DOI: https://doi.org/10.1134/S1061830919110068.

[22] Y. Gaoa et al. "Multiple cracks detection and visualization using magnetic fluxleakage and eddy current pulsed thermography.". *Sens. Actuators A Phys*, 2015.
DOI: https://doi.org/10.1016/j.sna.2015.09.011.

[23] A. Sophian, G. Y. Tian, and Zairi S. "Pulsed magnetic flux leakage techniques for crack detection and characterization. ". *Sens. Actuator A.*, 2006.
DOI: https://doi.org/10.1016/j.sna.2005.07.013.

[24] D. Kim, L. Udpa, and S. Udpa. "Remote field eddy current testing for detection of stress corrosion cracks in gas transmission pipelines.". *Materials Letters*, 2004.
DOI: https://doi.org/10.1016/j.matlet.2004.01.006.

[25] A. Akbari-Khezri and H. Hesamedin. "Determination of Crack Depth Profile in Cylindrical Metallic Structures, Using Alternating Current Field Measurement Data.". *Journal of Nondestructive Evaluation*, 2019.
DOI: https://doi.org/10.1007/s10921-019-0596-3.

[26] W. Dehui, L. Zhitian, W. Xiaohong, and S. Lingxin. "Composite magnetic flux leakage detection method for pipelines using alternating magnetic field excitation.". *NDT and E International*, 2017.
DOI: https://doi.org/10.1016/j.ndteint.2017.07.002.

[27] R. Wang, Y. Kang, et al. "A Novel Magnetic Flux Leakage Testing Method Based on AC and DCComposite Magnetization.". *Journal of Nondestructive Evaluation*, 2020.
DOI: https://doi.org/10.1007/s10921-020-00730-0.

[28] C. Alexander and M. Sadiku. "Fundamentals of electric circuits. ". 3th ed. McGraw-Hill Inc. New York, 2006.

[29] J. Nagel. "Induced Eddy Currents in Simple Conductive Geometries: Mathematical Formalism Describes the Excitation of Electrical Eddy Currents in a Time-Varying Magnetic Field.". *IEEE Antennas and Propagation Magazine*, 2018.
DOI: https://doi.org/10.1109/MAP.2017.2774206.